

---

# Silicon inhibition effects on the polymerase chain reaction: A real-time detection approach

---

Wei Wang,<sup>1</sup> Hai-Bin Wang,<sup>2</sup> Zhi-Xin Li,<sup>1</sup> Zeng-Yuan Guo<sup>1</sup>

<sup>1</sup>Department of Engineering Mechanics, Tsinghua University, Beijing 100084, People's Republic of China

<sup>2</sup>The No. 302 Hospital, Beijing 100039, People's Republic of China

Received 24 May 2005; revised 31 August 2005; accepted 31 August 2005

Published online 12 December 2005 in Wiley InterScience (www.interscience.wiley.com). DOI: 10.1002/jbm.a.30627

**Abstract:** In the miniaturization of biochemical analysis systems, biocompatibility of the microfabricated material is a key feature to be considered. A clear insight into interactions between biological reagents and microchip materials will help to build more robust functional bio-microelectromechanical systems (BioMEMS). In the present work, a real-time polymerase chain reaction (PCR) assay was used to study the inhibition effects of silicon and native silicon oxide particles on Hepatitis B Virus (HBV) DNA PCR amplification. Silicon nanoparticles with different surface oxides were added into the PCR mixture to activate possible interactions between the silicon-related materials and the PCR reagents. Ratios of silicon nanoparticle surface area to PCR mixture volume (surface to volume ratio) varied from 4.7 to 235.5 mm<sup>2</sup>/μL. Using high speed centrifugation, the nanoparticles were pelleted to tube inner surfaces. Supernatant extracts were then used in subsequent PCR experiments. To

test whether silicon materials participated in amplifications directly, in some cases, entire PCR mixture containing silicon nanoparticles were used in amplification. Fluorescence histories of PCR amplifications indicated that with the increase in surface to volume ratio, amplification efficiency decreased considerably, and within the studied ranges, the higher the particle surface oxidation, the stronger the silicon inhibition effects on PCR. Adsorption of Taq polymerase (not nucleic acid) on the silicon-related material surface was the primary cause of the inhibition phenomena and silicon did not participate in the amplification process directly. © 2005 Wiley Periodicals, Inc. *J Biomed Mater Res* 77A: 28–34, 2006

**Key words:** real-time PCR; inhibition effects; silicon; nanoparticles

---

## INTRODUCTION

Polymerase chain reaction (PCR), which is a thermally activated chemical reaction for nucleic acid amplification, is one of the most important molecular biological methods.<sup>1</sup> The number of nucleic acids will be doubled after one thermal cycle by controlling the sample and reagent temperature in sequence to the denaturation temperature, the annealing temperature, and the extension temperature with transitions. After several tens of cycles, the amplified nucleic acids in the PCR mixture will be rich enough for further detection and analysis. It has been demonstrated experimentally that the time spent in temperature transitions was

usually wasted and the transition time after the extension and the denaturation periods had no function.<sup>2</sup> Furthermore, nonspecific amplification can be minimized with a rapid denaturation temperature to annealing temperature transition.<sup>3</sup> Therefore, in the past decade, development of a PCR instrument with rapid temperature ramping, that is, rapid PCR, has become an area of significant interest.

It is well known that characteristic time of thermal transportation in a given device is direct proportional to the second power of the device size. Therefore, a thermal cycling instrument with characteristic size in microscale is a perfect candidate to realize the rapid PCR. With the development of silicon microfabrication techniques, silicon-based micro-PCR chips have been widely studied to achieve rapid PCR as well as reducing the power consumption and the required space.<sup>4–11</sup> Silicon offers many substantial advantages in establishing PCR instruments, such as very high thermal conductivity and ease of fabrication. However, the use of silicon in micro-PCR chips poses some drawbacks, especially in terms of the biocompatibility issue. The high surface to volume ratio increases the

Correspondence to: W. Wang, Institute of Microelectronics, Peking University, Beijing 100871, People's Republic of China; e-mail: w.wang@pku.edu.cn

Contract grant sponsor: Scientific Research Innovation Foundation of Tsinghua University

Contract grant sponsor: National Natural Science Foundation of China; contract grant number: 59995550–2

importance of the surface chemistry on the biological operations in these micro devices.<sup>12</sup>

Native silicon was found to be an inhibitor of PCR and nucleic acids amplification in an untreated silicon-based PCR chip had a high failure rate.<sup>13</sup> To render the inner surface of silicon-based micro-PCR chips, surface passivation procedures have been developed, which can be classified into two types: static passivation and dynamic passivation.<sup>14</sup> Static passivation means that before performing PCR, the surface is treated by oxidizing silicon<sup>4,6,9-11</sup> or by silanizations,<sup>5,8</sup> while the dynamic approach refers to adding the passivating agents directly into the PCR mixture.<sup>7,8,10,14</sup> Early studies revealed that passivating the silicon surfaces with a silanizing agent followed by a polymer treatment can result in a good amplification but the yields were inconsistent within the different treatments and were not always comparable with PCR in the conventional tubes.<sup>13</sup> Further research indicated that silanization of SiO<sub>x</sub> surfaces alone will not be suitable for multiple PCR or long-term application because of degradation of the surface-passivating organic film.<sup>15</sup> Most dynamic coatings performed for silicon-based PCR chips have used bovine serum albumin (BSA) as the passivating agent. It has been found that in conventional amplification experiments, high concentrations of BSA caused lower yields than controls (without BSA added) and amplification could even be shut down at a very high BSA concentration.<sup>6</sup> Hence, a given PCR reaction in silicon-based microchip should be optimized in advance to find the optimal BSA concentration. Among the passivating methods, thermally oxidized silicon surfaces were demonstrated to be compatible with PCR to give consistent amplifications when compared with reactions performed in conventional PCR tubes.<sup>13</sup>

As for the inhibition mechanism, more and more data suggest that the inhibition of PCR by silicon-related materials is mainly due to the adsorption of the Taq polymerase and/or the nucleic acid onto the chip inner surfaces and not from a straight chemical action.<sup>6,15,16</sup>

In experiments reported for analysis of silicon inhibition effects on PCR, the PCR amplification results were all detected by gel electrophoreses.<sup>13-16</sup> This off-chip manual operation increases the potential for cross contamination, and the additional post-PCR step can only provide a qualitative insight into the inhibition phenomena. This implies that the different gel band fluorescence intensities in the electrophoresis cannot be simply taken as evidence of inhibition effects. In the recent past, real-time PCR-based assay has become an invaluable tool for many scientists working in different disciplines, especially in the field of molecular diagnostics. The real-time PCR technique was characterized by a wide dynamic range of quantification, a

high sensitivity and high precision.<sup>17,18</sup> No post-PCR steps required minimizes risks of cross contamination.

The aim of the present work was to provide a quantitative insight into silicon substrate inhibition effects on polymerase chain reaction by a real time PCR approach. Two kinds of silicon nanoparticles with different oxidation states at their surfaces were used as experimental silicon materials. Reactions between the silicon-related materials and the PCR mixture were evoked by mixing the silicon nanoparticles with the PCR reagents, and subsequently stopped by a high speed centrifugation to sedimentate the nanoparticles onto the inner surface of the experimental tubes. Fluorescence histories of the real-time detection were used to evaluate the inhibition effect and to explore its mechanism.

## MATERIALS AND METHODS

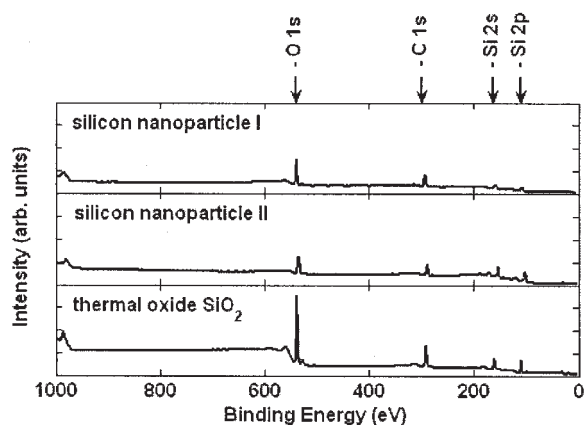
### Silicon particulate materials

To minimize the parasitic thermal mass introduced by the additional silicon materials, sol-gel prepared silicon nanoparticles with a nominal diameter ranging from 20 to 50 nm (ZhongChao Nano, China) have been used as the test materials in the present experiments. Two kinds of silicon nanoparticles were examined: (1) silicon nanoparticle exposed in the air for a long time with a native oxide layer formed on its surface, named as silicon nanoparticle I hereafter, and (2) nonoxidized silicon nanoparticles which were taken out from a nitrogen protected bottle just before experiments, named as silicon nanoparticle II.

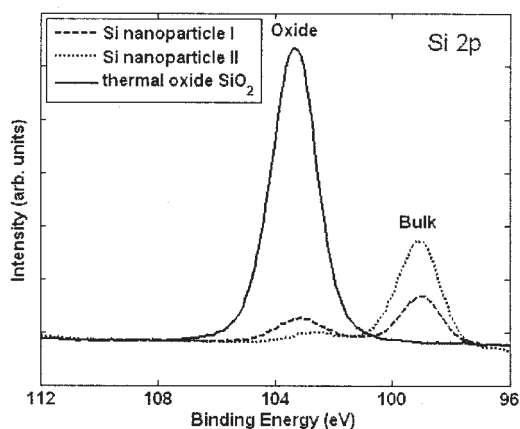
X-ray photoelectron spectroscopy (XPS, PHI-5300 ESCA™, PerkinElmer, USA) was used to evaluate the surface oxidation degree of the two nanoparticles by measuring the spectra of the two nanoparticles, compared with a silicon wafer with a thick thermal oxide layer (fabricated by standard industrial thermal oxidation process in Hebei Semiconductor Research Institute, Shijiazhuang, China; thickness of its oxide layer was larger than 110 nm). An aluminium anode was used as source, operating at 250 W. The binding energies were lined up with respect to the C1s peak at 285 eV. Wide-scan spectra for the three samples are illustrated in Figure 1(A). Si2p high resolution spectra for the three samples, as shown in Figure 1(B), indicate a clear Si2p peak at 103.3 eV in the nanoparticle-I spectrum, signifying that the nanoparticle-I was slightly oxidized. Mean while, XPS of nanoparticle-II exhibits a very weak Si2p peak at 103.3 eV, but a distinct one at 99.3 eV. No Si2p peak at 99.3 eV for the thermal oxide SiO<sub>2</sub> sample was detected because the thickness of its oxide layer was much larger than the inelastic mean free path of XPS. Thickness of the silicon oxide overlayer can be calculated from the spectrum by using the following equation<sup>19</sup>

$$t_{\text{ox}} = \lambda_{\text{SiO}_2} \sin \theta \left\{ \frac{I_{\text{SiO}_2}^{\text{exp}} / I_{\text{Si}}^{\text{exp}}}{\beta} + 1 \right\} \quad (1)$$

where  $\theta$  was the angle between the sample surface plane and the electron analyzer,  $\lambda_{\text{SiO}_2}$  was the attenuation length of the



(A)



(B)

**Figure 1.** XPS spectra for the two silicon nanoparticles with a thermal oxide silicon wafer. (A) Wide-scan spectra for the three samples, (B) Si2p high resolution spectra for the three samples (selected data from panel A).

Si2p photoelectrons in SiO<sub>2</sub>, and  $\beta$  was the ratio of the Si2p intensity from infinitely thick SiO<sub>2</sub> to that of Si. In the present experiments,  $\theta$  was 45°, and as recommended by Shallenberger et al.<sup>20</sup>  $\lambda_{\text{SiO}_2}$  and  $\beta$  were taken as 2.7 nm and 0.83, respectively. Therefore, the thickness of the native silicon oxide films of the nanoparticle I and II were calculated to be about 3.33 and 2.52 nm, respectively.

The specific surface area (surface area per unit mass) of the two kinds of nanoparticles were measured by Brunauer–Emmet–Teller adsorption method (BET, NOVA4000™, Quantachrome, USA). On the basis of nitrogen adsorption, the specific surface area of the silicon nanoparticle I was 47.63 m<sup>2</sup>/g and that of the nanoparticle II was 77.83 m<sup>2</sup>/g.

To guarantee that the silicon-related material surface areas in the individual experimental tubes were the same; 3.9 mg of silicon nanoparticle I and 2.4 mg silicon nanoparticle II were added into two tubes with 1 mL sterile water, respectively. The ratio of silicon surface area to volume of each

nanoparticle-suspended liquid was  $186 \pm 0.8 \text{ mm}^2/\mu\text{L}$ . Mastersizer 2000™ (Malvern Instruments, UK) was used to evaluate the cluster degree of the two kinds of nanoparticle-suspended liquids. Results showed that the average diameters of nanoparticle I and II clusters in sterile water were 399 and 297 nm, respectively.

## PCR Protocol

In the present experiments, the amplification target was DNA of Hepatitis B Virus (HBV, clinical samples provided by No. 302 Hospital), and the buffer in the present experiment contained 10 mM Tris–HCl, pH 8.3, 50 mM KCl, 3.5 mM MgCl<sub>2</sub>, 400 mM dUTP, 200 mM each dATP, dCTP, and dGTP, 300 nM each primer, and 200 nM probe (Shanghai Sangon Co., China). The sequence for the forward primer was 5′-ATC CTG CTG CTA TGC CTC ATC TT-3′, and the sequence for the reverse one was 5′-ACA GTG GGG GAA AGC CCT ACG AA-3′ (Shanghai Sangon Co., China). Together, these two primers define a 103 bp PCR product. For homogeneous detection using the TaqMan™ system, a fluorescent probe was also included. The sequence of the HBV-DNA fluorescent probe was 5′-R-TGG CTA GTT TAC AGT GCC ATT TG-Q-3′ (Shanghai Sangon Co., China), where R was the fluorescent reporter dye and Q was the fluorescent quencher dye.

In ilka amplification, the PCR mixture containing 35  $\mu\text{L}$  buffer, 0.5  $\mu\text{L}$  Taq polymerase (1.25 U/ $\mu\text{L}$  AmpliTaq Gold DNA polymerase, PerkinElmer), and 4  $\mu\text{L}$  DNA template (extracted and purified from the clinical sample by QIAamp DNA Blood Mini Kit™, Qiagen, USA) was mixed with the silicon nanoparticles (volume ignored) as described in the following section. The pre-denaturation period was 95°C for 120 s, and then 35 cycles of amplification were performed using a thermal profile of 94°C for 20 s and 53°C for 30 s. The amplifications were carried out in a real-time PCR instrument, Slan™ (Hong Shi, China).

## Experimental procedures

To evaluate the silicon inhibition effects on HBV DNA amplification, an experiment was designed, which is referred as “inhibition experiment” hereafter. First, the two silicon nanoparticle-suspended liquids were oscillated to homogeneity. Then, 1, 2, 5, 10, 20, and 50  $\mu\text{L}$  of the two liquids was distributed into 12 tubes, respectively. A 12,000 rpm (about 1000 $\times$ g) rotation for 3 min made the silicon nanoparticles partition to the inner surfaces in each tube. Supernatant was aspirated. The PCR mixture prepared beforehand was added into the 12 tubes, and then oscillated with the pelleted silicon nanoparticles to regenerate a homogeneous nanoparticles suspension. The liquid was then allowed to stand for 3 min to make the reagents contact the silicon nanoparticles adequately. Another 3-min 12,000 rpm rotation was used to separate the nanoparticles from the PCR mixture and was treated as a stopping “reagent” of the possible reaction between the PCR reagents and the silicon-related materials. The supernatants were extracted again and injected into another 12 fresh tubes. These 12

TABLE I  
PCR Mixture Preparation in Mechanism Experiments

	Tube 1	Tube 2	Table 3	Tube 4
Silicon nanoparticles	I	I	I	I
Adsorption objects	Enzyme + buffer	Enzyme + buffer	Template + buffer	Template + buffer
Adding reagent	Template	Template	enzyme	enzyme
Silicon remaining	Yes	No	Yes	No

test samples with 2 positive controls (without silicon nanoparticles) and 1 negative control (without the HBV DNA template) were thermally cycled in the **Slan™ real-time PCR instrument**.

Another experiment (“mechanism experiment”) was designed and carried out to distinguish the reactive reagent in the PCR mixture with the two kinds of silicon nanoparticles and to test whether the silicon material participated in the nucleic acid amplification directly. First, prepared nanoparticle I suspended samples were oscillated to homogeneity and dispersed into 4 tubes, each tube with 50  $\mu\text{L}$  volume. Rotation for 3 minutes at 12,000 rpm was used to pellet the nanoparticles to the tube inner surface, and then supernatants were extracted from the tubes. Template–buffer or enzyme–buffer mixtures were added into the different numbered tubes as illustrated in Table I. The added reagents and sedimented nanoparticles were oscillated to homogeneity again, and stabilized for 20 min to allow the reaction between the silicon materials and the PCR mixture progress completely. Another 12,000 rpm rotation pelleted the silicon nanoparticles to the tube inner surfaces, and then the absent reagent (template or enzyme) was injected into each tube. Supernatants in Tubes 2 and 4 were extracted and injected into two fresh tubes, respectively, and the following amplifications were performed without silicon nanoparticles. The other two tubes were placed into the **Slan™ PCR instrument** directly with the nanoparticles inside for PCR amplification. The parasitic thermal mass effect introduced by the additional silicon nanoparticles was neglected because the thermal mass of silicon nanoparticles inside tube was only about 0.19% of that of the PCR mixture. The four test tubes were amplified simultaneously with 2 positive controls (without silicon nanoparticles) and 1 negative control (without the HBV DNA template) in the **Slan™ real-time PCR instrument**.

Assay repeatability was tested and the results indicated that the **Slan™ real-time PCR instrument** can provide a robust and reliable nucleic acid amplification (data not shown).

## RESULTS AND DISCUSSION

### PCR inhibition performance

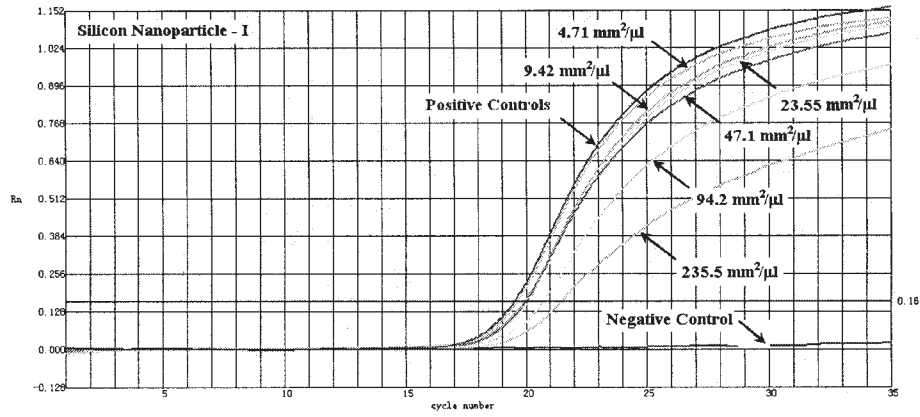
In the inhibition experiment, fluorescence histories in the 15 experimental tubes (12 samples, 2 positive controls, and 1 negative control) for tubes containing silicon nanoparticle I and silicon nanoparticle II were shown in Figure 2. The real-time fluorescence records indicated that regardless of the oxidation degree of the nanoparticles surfaces, the existence of silicon-related materials in the PCR mixture preparation procedure always re-

sulted in an amplification efficiency reduction. And with the increase in the particle surface to volume ratio, the fluorescence intensities in amplification decreased considerably. As shown in Figure 2(C), in the experiments using silicon nanoparticle I (surface to volume ratio of  $235.5 \text{ mm}^2/\mu\text{L}$ ), fluorescence intensity in the tube at the 35th cycle was about 66% of that of the positive control, while in the experiments with silicon nanoparticle II, the factor was about 83%. Results indicate that the higher oxidized silicon surface (native oxide on silicon nanoparticle I) exhibited a much stronger inhibition effect on the HBV DNA amplification. This conclusion seemed inconsistent with previous results<sup>14–16</sup>, claiming that the silicon oxide was compatible with PCR but pure unoxidized silicon was not.

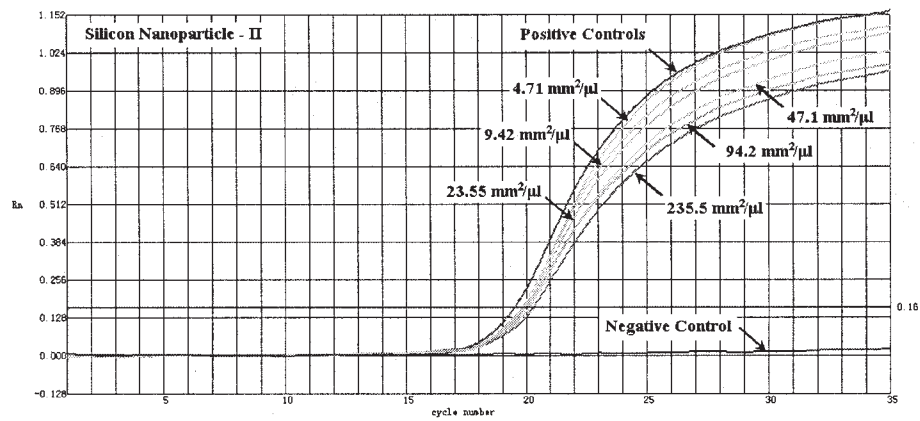
These apparent contradicting phenomena can be attributed to variations of silanol (active site) densities at the surface with different oxidation degrees and thermal treatment methods. Silanol surface was reported to be able to adsorb proteins considerably,<sup>21</sup> and Taq polymerase adsorption on surface was proposed to be the primary cause for silicon inhibition effects on PCR as discussed in the next section. For naked silicon, the surface has a low oxygen concentration and presents a very small number of hydroxyl sites, while the natural oxidation produces a Si—O surface, which is easily oxidized to silanols in aqueous solution. Preparations of PCR-compatible silicon oxides in the previous works usually include a very high temperature thermal treatment (ca.  $1000^\circ\text{C}$ ). This high temperature oxidization process makes silicon surface in the form of O—Si—O and stable against the hydrolysis processes.<sup>22</sup> Therefore, the hydroxide (silanol) is difficult to form on the surface.

### Inhibition mechanism

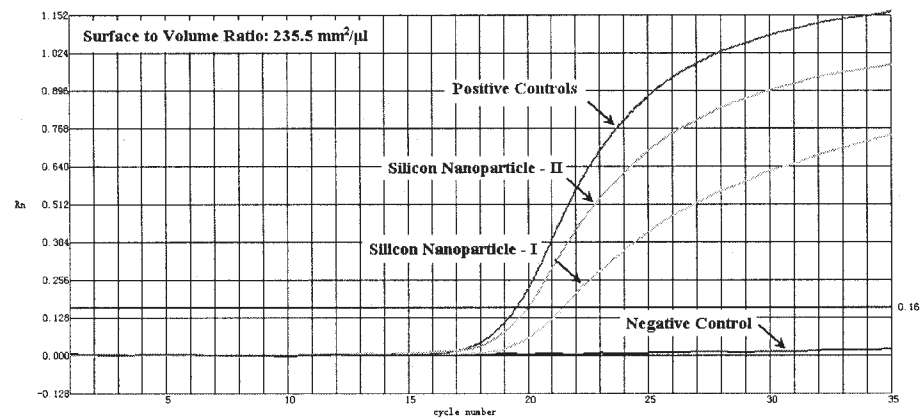
Fluorescence histories comparing the amplifications with DNA adsorption tests and Taq polymerase adsorption tests in the mechanism experiments with silicon nanoparticle I (surface to volume ratio of  $235.5 \text{ mm}^2/\mu\text{L}$ ) are shown in Figure 3(A). Amplification efficiencies decreased considerably in the Taq polymerase adsorption test, and fluorescence intensity in the tube at the 35th cycle was about 64% of that of the positive control, while in the DNA adsorption test, the



(A)

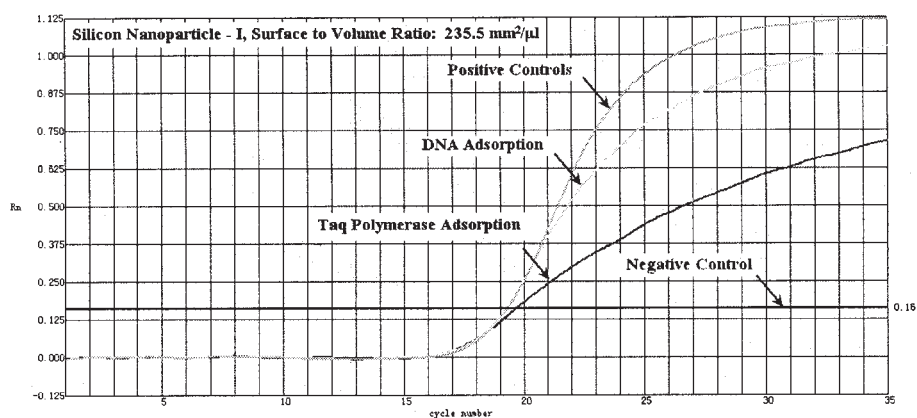


(B)

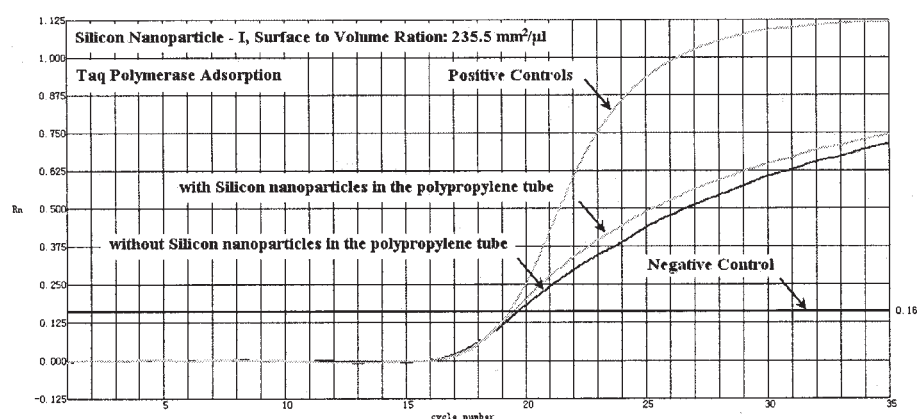


(C)

**Figure 2.** Fluorescence histories of HBV-DNA amplifications with different surface to volume ratios in inhibition experiment (with 2 positive controls and 1 negative control). (A) Results for silicon nanoparticle I, (B) results for silicon nanoparticle II, and (C) comparison of fluorescence histories of silicon nanoparticle I and II with a surface to volume ratio of  $235.5 \text{ mm}^2/\mu\text{L}$  (selected data from panels A and B).



(A)



(B)

**Figure 3.** Fluorescence histories of the HBV-DNA amplifications in mechanism experiment (with 2 positive controls and 1 negative control). (A) Results of amplifications in DNA adsorption tests and Taq polymerase adsorption tests with silicon nanoparticle I (surface to volume ratio of  $235.5 \text{ mm}^2/\mu\text{L}$ ). (B) Results of amplifications with and without silicon nanoparticles (silicon nanoparticle I with a surface to volume ratio of  $235.5 \text{ mm}^2/\mu\text{L}$ ) in Taq polymerase adsorption tests.

factor was about 92%. Ct values, the threshold cycle number at which fluorescence begins to increase rapidly, usually a few standard deviations above the baseline, in the both tests did not shift, as illustrated in Figure 3(A). Because the plot of Ct value versus template number is linear in the real time PCR assay, the observed non Ct value-shift means that there is no detectable DNA adsorption on the silicon nanoparticles. Results demonstrated that the observed inhibition effects can be attributed to the adsorption of the Taq polymerase on the silicon oxide surface and that the adsorption of the template (DNA) is not a primary factor. Amplification results for nanoparticle II are the same as those for nanoparticles I (data not shown), except that the intensities of the inhibition are different. This is also the same as those found in gel electrophoresis detection.<sup>23</sup>

By controlling the silicon nanoparticles remaining in the thermal cycling process, the straight inhibition phenomena on PCR was tested. Fluorescence histories of PCR amplifications with and without silicon nanoparticles (silicon nanoparticle I, surface to volume ratio of  $235.5 \text{ mm}^2/\mu\text{L}$ ) in the Taq polymerase adsorption tests are shown in Figure 3(B). It is clear that under these two kinds of conditions, the nucleic acid amplification efficiencies remain nearly the same. Similarly, amplifications with and without silicon nanoparticles in the DNA adsorption tests have the same efficiencies (Data not shown).

We conclude that silicon nanoparticles have no direct inhibition effects on the PCR amplification and the inhibition phenomena should be ascribed to the adsorption of the Taq polymerase on the silicon related material surface.

## CONCLUSIONS

As a mature fabrication material used in the MEMS, silicon has been widely used to fabricate miniaturized PCR devices. However, in the silicon-based micro-PCR chips, surface chemistry plays an important role in nucleic acid amplification. We have shown that silicon produces a detectable inhibition on the PCR reaction, confirming previous works.

In the present work, a real-time polymerase chain reaction assay was used to provide a quantitative insight into this inhibition phenomenon. In the experiments, silicon based nanoparticles with high specific areas were mixed with the PCR mixture to evoke interaction between them. A broad range of surface analysis techniques including X-ray photoelectron spectroscopy and Brunauer–Emmet–Teller adsorption isotherms were used to characterize the two nanoparticles before the experiments. In PCR experiments, ratios of the silicon/silicon oxide surface area to the PCR mixture volume varied from 4.71 to 235.5 mm<sup>2</sup>/μL. Fluorescence intensities detected by the real-time PCR instrument indicated that with the increase in surface to volume ratio, the amplification efficiency decreased considerably, and particles with native oxide exhibited a much greater inhibition effect on nucleic acid amplification than naked silicon particles. Enhanced PCR inhibition phenomena were attributed to the very large number of surface silanol groups present on the native oxide surface. Experimental results suggested that the adsorption of Taq polymerase (not nucleic acid) onto the silicon surface was the primary cause of the PCR inhibition and silicon did not participate in the amplification process.

The next phase of this work will scrutinize the inhibition effects of other silicon-related materials, including silicon nitride, silicon dioxide (wet oxidation, dry oxidation, and chemical vapor deposited oxidation), polysilicon, and other materials. Further studies on the adsorption of Taq-polymerase on the microfabricated surface will also be a focus.

## References

- Mullis KB, Ferré F, Gibbs RA. *The Polymerase Chain Reaction*, Birkhäuser: Boston; 1994.
- Wittwer CT, Fillmore GC, Garling DJ. Minimizing the time required for DNA amplification by efficient heat transfer to small samples. *Anal Biochem* 1990;186:328–331.
- Wittwer CT, Garling DJ. Rapid Cycle DNA amplification: Time and temperature optimization. *Biotechniques* 1991;10:76–83.
- Cheng J, Shoffner MA, Hvichia GE, Kricka LJ, Wilding P. Investigation of different PCR amplification systems in microfabricated silicon-glass chips. *Nucleic Acids Res* 1996;24:380–385.
- Poser S, Schulz T, Dillner U, Baier V, Köhler JM, Schimkat D, Mayer G, Siebert A. Chip elements for fast thermal cycling. *Sensor Actuators A* 1997;62:672–675.
- Taylor TB, Winn-Deen ES, Picozza E, Woudenberg TM, Albin M. Optimization of the performance of the polymerase chain reaction in silicon-based microstructure. *Nucleic Acids Res* 1997;25:3164–3168.
- Daniel JH, Iqbal S, Millington RB, Moore DF, Lowe CR, Leslie DL, Lee MA Pearce MJ. Silicon DNA microchambers for DNA amplification. *Sensor Actuators A* 1998;71:81–88.
- Schneegaß I, Bräutigam R, Köhler JM. Miniaturized flow-through PCR with different template types in a silicon chip thermocycler. *Lab on a Chip* 2001;1:42–49.
- Lee DS, Park SH, Yang H, Chung KH, Yoon TH, Kim SJ, Kim K, Kim YT. Bulk-micromachined submicroliter-volume PCR chip with very rapid thermal response and low power consumption. *Lab on a Chip* 2004;4:401–407.
- Matsubara V, Kerman H, Kobayashi M, Yamamura S, Morita V, Takamura Y, Tamiya E. On-chip nanoliter-volume multiplex TaqMan polymerase chain reaction from a single copy based on counting fluorescence released microchambers. *Anal Chem* 2004;76:6434–6439.
- Krishnan M, Burke DT, Burns MA. Polymerase chain reaction in high surface-to-volume ratio SiO<sub>2</sub> microstructures. *Anal Chem* 2004;76:6588–6593.
- de Mello AJ. DNA amplification: does ‘small’ really mean ‘efficient’? *Lab on a Chip* 2001;1:24N–29N.
- Shoffner MA, Cheng J, Hvichia GE, Kricka LJ, Wilding P. Chip PCR. I. Surface passivation of microfabricated silicon-glass chips for PCR. *Nucleic Acids Res* 1996;24:375–384.
- Lou XJ, Panaro NJ, Wilding P, Fortina P, Kricka LJ. Increased amplification efficiency of microchip-based PCR by dynamic surface passivation. *Biotechniques* 2004;36:248–252.
- Felbel J, Bieber I, Pipper J, Köhler JM. Investigations on the compatibility of chemically oxidized silicon (SiO<sub>x</sub>)-surface for applications towards chip-based polymerase chain reaction. *Chem Eng J* 2004;101:333–338.
- Erill I, Campoy S, Erill N, Barbé J, Aguiló J. Biochemical analysis and optimization of inhibition and adsorption phenomena in glass-silicon PCR-chips. *Sensor Actuators B* 2003; 96:685–692.
- Schmittgen TD. Real-time quantitative PCR. *Methods* 2001;25: 383–385.
- Klein D. Quantification using real-time PCR technology: Applications and limitations. *Trends Mol Med* 2002;8:257–260.
- Hill JM, Royce DG, Fadley CS, Wagner LF, Grunthaler FJ. Properties of oxidized silicon determined by angle-dependent X-ray photoelectron spectroscopy. *Chem Phys Lett* 1976;44:225.
- Cole DA, Shallenberger JR, Novak SW, Moore RL, Edgell MJ, Smith SP, Hitzman CJ, Kirchhoff JF, Principe E, Nieveen W, Huang FK, Biswas S, Bleiler RJ, Jones K. Oxide thickness determination by XPS, AES, SIMS, RBS and TEM. *J Vac Sci Technol B* 2000;18:440–444.
- Alcantar NA, Aydil ES, Israelachvili JN. Polyethylene glycol-coated biocompatible surface. *J Biomed Mater Res* 2000;51:343–351.
- Dugas V, Chevalier Y. Surface hydroxylation and silane grafting on fumed and thermal silica. *J Colloid Interface Sci* 2003; 264:354–361.
- Wang W, Wang HB, Li ZX, Guo ZY. Studies of silicon inhibition effects on polymerase chain reaction. *China Biotechnology* 2005;25(3):69–73.